

断层几何结构与物理场的 演化及失稳特征*

马 瑾 马胜利 刘力强 邓志辉 马文涛 刘天昌

(中国北京 100029 国家地震局地质研究所)

摘要 在双轴加载条件下,研究了几种具不同几何结构的断层系变形破坏过程中应变、断层位移和声发射事件的时空分布,并对典型失稳事件的特征进行了分析.研究表明:具不同几何结构的断层系有不同的变形物理场演化图象;根据物理场演化特征和变形机制的差异,可识别出两类粘滑型失稳、破裂型失稳及混合型失稳,不同类型的失稳在前兆上有明显差异;失稳类型与断层几何结构及变形阶段密切相关.因此,研究自然界断层的几何结构,对地震预报和地震前兆观察研究极为重要.

主题词 岩石力学实验 断层组合 声发射 应变 断层位移

引言

浅源地震与地壳中断层的活动密切相关.在大多数情况下,断层并不是简单连续的面状构造,而是复杂不连续的断裂组合带.理论分析表明,断层几何结构的非连续会引起应力场的复杂变化(Segall, Pollard, 1980);实际震例表明,地震破裂的成核、扩展以及终止常受断层几何结构的影响(Sibson, 1986; Scholz, 1990);断层几何结构的复杂性使得变形破坏过程复杂化,必然引起地震前兆分布的复杂性(马瑾, 1987).因此,研究具不同几何结构的断层系的变形破坏及物理场演化过程,对理解地震机制和前兆是很有意义的.由于构造运动是十分缓慢的过程,仅依赖于野外观测资料,常难以了解断层的变形及物理场演化过程.而岩石力学模拟实验可在此方面提供有价值的参考资料.

对平直断层(Dieterich *et al.*, 1978; Mogi, 1984; 马瑾, 1987)、雁列断层(刘力强等, 1986; 李建国等, 1989; 张之立, 李强, 1993)、“人”字型(杜异军等, 1991)及其它典型断层组合(马瑾, 1987)变形过程中应变、断层位移、声发射等物理场的演化都曾进行过实验研究,从中可以看出断层几何结构对破坏方式和前兆分布等的影响.但从加载方式来看,许多实验是在单轴条件下进行的,未能揭示变形破坏的全过程;从物理场观测手段来看,大多数实验采用的是模拟记录,观测的精度和速度及观测项目的综合性都很有限.近年来在利用多通道数字式观测设备研究断层变形物理场(前兆场)方面取得了一些新结果(大中康誉等, 1993; 佐藤隆司等, 1993; 加藤尚之等, 1993),但断层模型较为简单.因此,对断层几

* 国家地震局“八五”攻关课题.

1995-11-03 收到初稿, 1995-11-14 决定采用.

何与物理场演化及失稳前兆关系的深入理解仍需大量的实验结果.

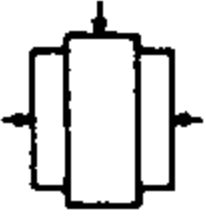
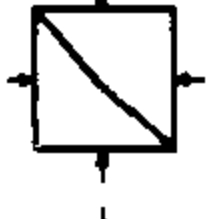
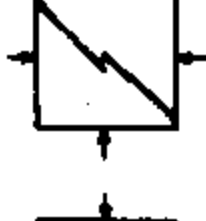
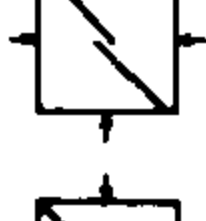
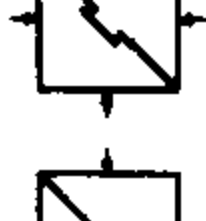

本文选择走滑断层带中常见的几种组合方式为实验模型, 利用一套高精度、多通道数字式测量系统, 在双轴加载条件下研究其变形破坏过程中应变场、断层位移场、声发射事件时空强分布的演化, 据此讨论断层几何结构与失稳类型及前兆特征的关系.

1 实验方法

实验采用的加载装置为一套双轴加载系统, 利用不同的压块组合可进行双剪实验、双轴摩擦实验及双轴压缩实验.

所研究的模型包括平直断层, 拐折断层, 挤压型、拉张型及由两者组合而成的雁列式断层以及共线非连续断层等. 各类标本特征、实验类型及实验条件汇于表 1.

表 1 标本结构、实验条件一览表

断层类型	标本结构	标本特征	实验条件
平直断层		花岗闪长岩, 人工研磨摩擦面, 滑动面积 28×5 cm	正应力 5~10 MPa, 位移速率 $1 \mu\text{m/s}$
拐折断层		辉长岩, $25 \times 25 \times 2$ cm, 含 5° 拐折, 人工研磨摩擦面	侧向应力 5~10 MPa, 轴向位移速率 $0.5 \mu\text{m/s}$
挤压型雁列断层		辉长岩, $25 \times 25 \times 2$ cm, 雁列区 2×2 cm, 断层带宽 3 mm, 石膏充填	侧向应力 5 MPa, 轴向压缩速率 $0.5 \mu\text{m/s}$
拉张型雁列断层		辉长岩, $25 \times 25 \times 2$ cm, 雁列区 2×2 cm, 断层带宽 3 mm, 石膏充填	侧向应力 5 MPa, 轴向压缩速率 $0.5 \mu\text{m/s}$
复杂雁列断层		两个雁列区, 辉长岩, $25 \times 25 \times 2$ cm, 雁列区 2×2 cm, 断层带宽 3 mm, 石膏充填	侧向应力 5 MPa, 轴向压缩速率 $0.5 \mu\text{m/s}$
共线非连通断层		辉长岩, $25 \times 25 \times 2$ cm, 非连通段 2.5 cm, 断层带宽 3 mm, 石膏充填	侧向应力 5 MPa, 轴向压缩速率 $0.5 \mu\text{m/s}$

实验中除对轴向载荷和轴向位移进行测量外, 在实验标本上布设了声发射传感器、应变片和断层位移计, 对相应的物理场进行观测.

声发射观测采用两套高速多通道(共 24 通道)测量系统. 根据声发射探头的全波形记录, 利用同一事件的到时差可确定其位置; 声发射强度的确定借鉴了计算地震震级的方法, 并考虑到声发射事件与地震之间的差别. 由此可得到每个标本变形过程中声发射 $M-t$ 图及时空分布图, 还可分析声发射事件的频谱、震源机制解等.

应变测量使用一套低频、高精度多点测量系统, 观测通道为 32 个, 传感器为标准应变片. 可直接利用单个应变片的测量记录给出所在部位及方向应变随时间的变化, 也可将相邻三个应变片组成一个应变花, 求出某一点平面主应变的大小、方向及随时间的变化. 断层位移观测使用的也是前述低频、高精度多点测量系统, 设置了 8 个断层位移计, 可直接利用每个通道的记录给出相应位置上断层位移的时程曲线.

2 实验结果

2.1 典型断层构造的变形过程及物理场演化

平直断层 以沿断层面的滑动为主(位移大), 应变积累限于断层面附近, 声发射事件

能量大但事件数目相对较少,摩擦阻力总体上处于稳态,物理场的演化也较平稳,只在失稳前后有明显的变化.

拐折断层 拐折的存在对断层活动有明显的阻碍作用,使得与轴向应力呈较小和较大角度的断层段交替成为主导活动构造.表现为断层位移变化相对较快,断层附近应变积累和释放较剧烈,声发射活动较强.拐折部位的声发射事件往往较小,主频较高,平直断层段上事件往往较大,主频较低.

雁列式断层 挤压型和拉张型两类雁列式断层具有类似的变形破坏过程,即:前期以雁列区内裂纹的产生、扩展、连通为主,应变变化剧烈而断层位移较小,声发射活动频度较高而能量相对较小;后期以沿断层带的滑动为主,断层位移明显,应变变化相对较小,声发射事件能量较大.但挤压型雁列区可积累较高的应变能,区内可发生较强的应变释放和声发射活动,且雁列区对滑动始终起着阻碍作用;而拉张型雁列式断层雁列区内难以产生快速的应变释放和较强的声发射活动,雁列区对后期的滑动无明显的阻碍作用.

复杂雁列式断层的变形过程及相应的物理场演化并非是两种雁列式断层的简单叠加,而是包含着它们之间的相互作用.其中一个有趣的现象是,能量较强的声发射事件主要分布在应力水平较低的张性雁列区附近的主干断层上,而不是应力水平较高的压性雁列区,但这种事件发生的时间则明显受控于压性雁列区的变形过程.

共线非连通断层 具有很高的强度,尽管断层端部可能会引起局部应力高度集中,但共线断层的扩展连通极为困难,其变形主要集中在非连通部位及邻近的断层上,以产生大量能量不高的声发射活动为特征.

2.2 失稳类型及前兆特征

实验中观察到具不同特征的失稳事件,根据其对应的变形机制和物理演化场特征,可分为粘滑型、破裂型和混合型失稳.失稳类型与断层几何结构有关,不同类型的失稳对应不同的失稳前兆特征.基于对典型失稳事件的分析,将各类失稳的特点及前兆特征简述如下.

粘滑型失稳 在断层滑动过程中出现的失稳,可见于平直断层、拐折断层的滑动中及雁列式断层雁列区贯通后的滑动中.从失稳前后物理场的演化特征来看,至少可识别出两类不同的失稳事件:一类失稳是断层在稳态滑动中由于滑动面状态的变化而造成局部闭锁,使得摩擦阻力上升,当应力增加到一定水平时,局部闭锁被打破,发生失稳扩展.基于断层摩擦本构关系,其机制可能属滑动弱化(Rice, 1980).这类失稳的前兆特征是:宏观应力上升,闭锁部位附近应变明显增加,断层位移速率下降,临近失稳时则有预滑现象.图1是平直断层摩擦滑动中这样一次失稳发生前后断层各段位移和应变的变化情况,粘滑发生前源区断层闭锁、应变增加及临近粘滑时的预滑(位移加快)现象均很明显;另一类失稳是断层在稳态滑动中由于整体加速或局部加速并快速扩展引起应力下降而造成的,其机制可能属速度弱化(Dieterich, 1979; Ruina, 1983).这类失稳难以观测到前兆.图2是断层摩擦滑动中一次失稳发生前后断层各段位移和应变的变化情况.失稳前仅见应变的瞬时增加,紧临失稳断层位移有加速扰动现象.

破裂型失稳 由断层带中强度较高的非连续部位次级断裂的扩展引起的失稳,可见于挤压型雁列区、共线非连续断层等部位,一般发生于变形初期.失稳前宏观应力上升,紧临失稳源区应变明显下降,而邻区应变上升.

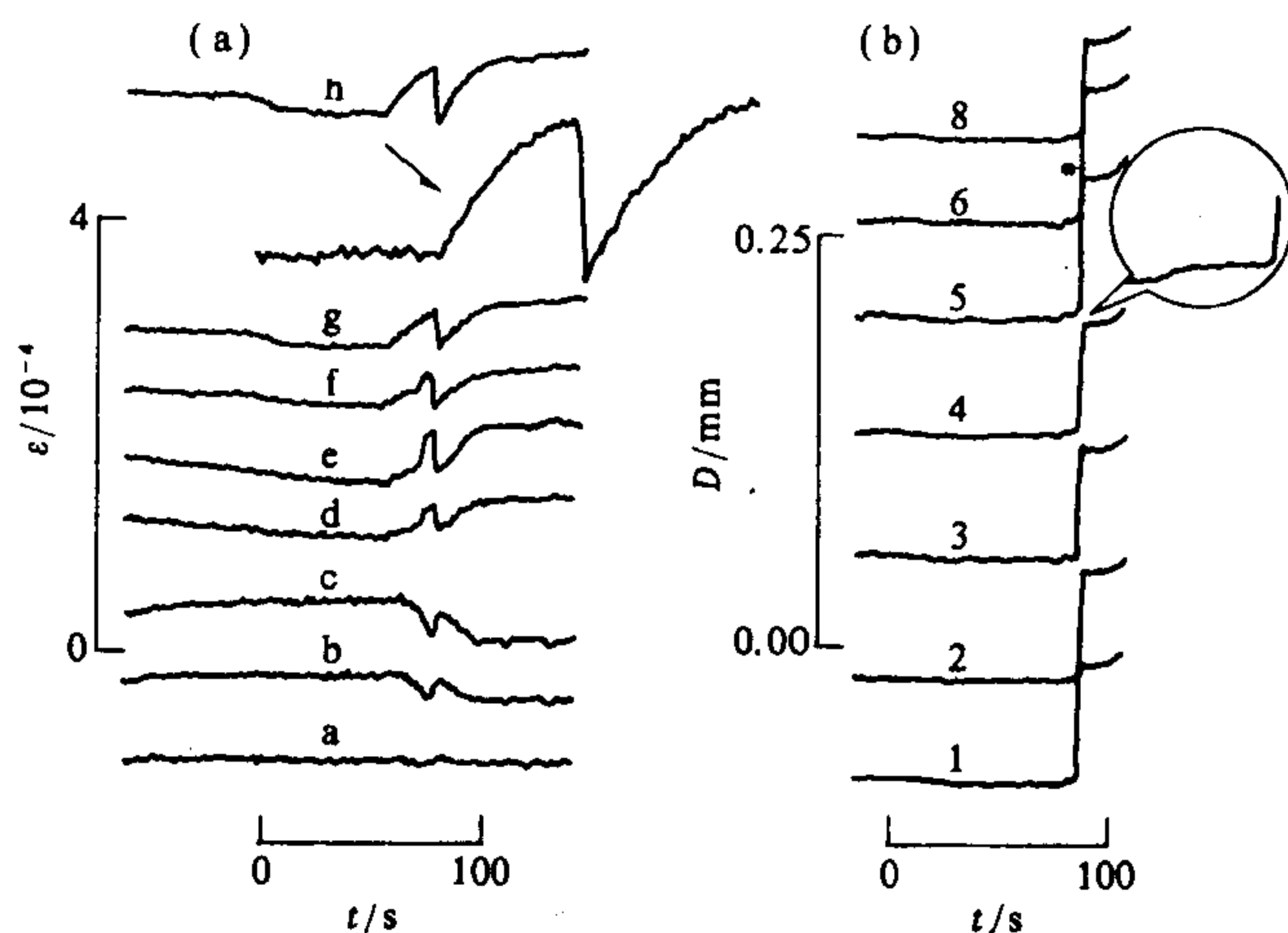


图 1 断层摩擦滑动中一种粘滑失稳前后应变和断层位移的变化

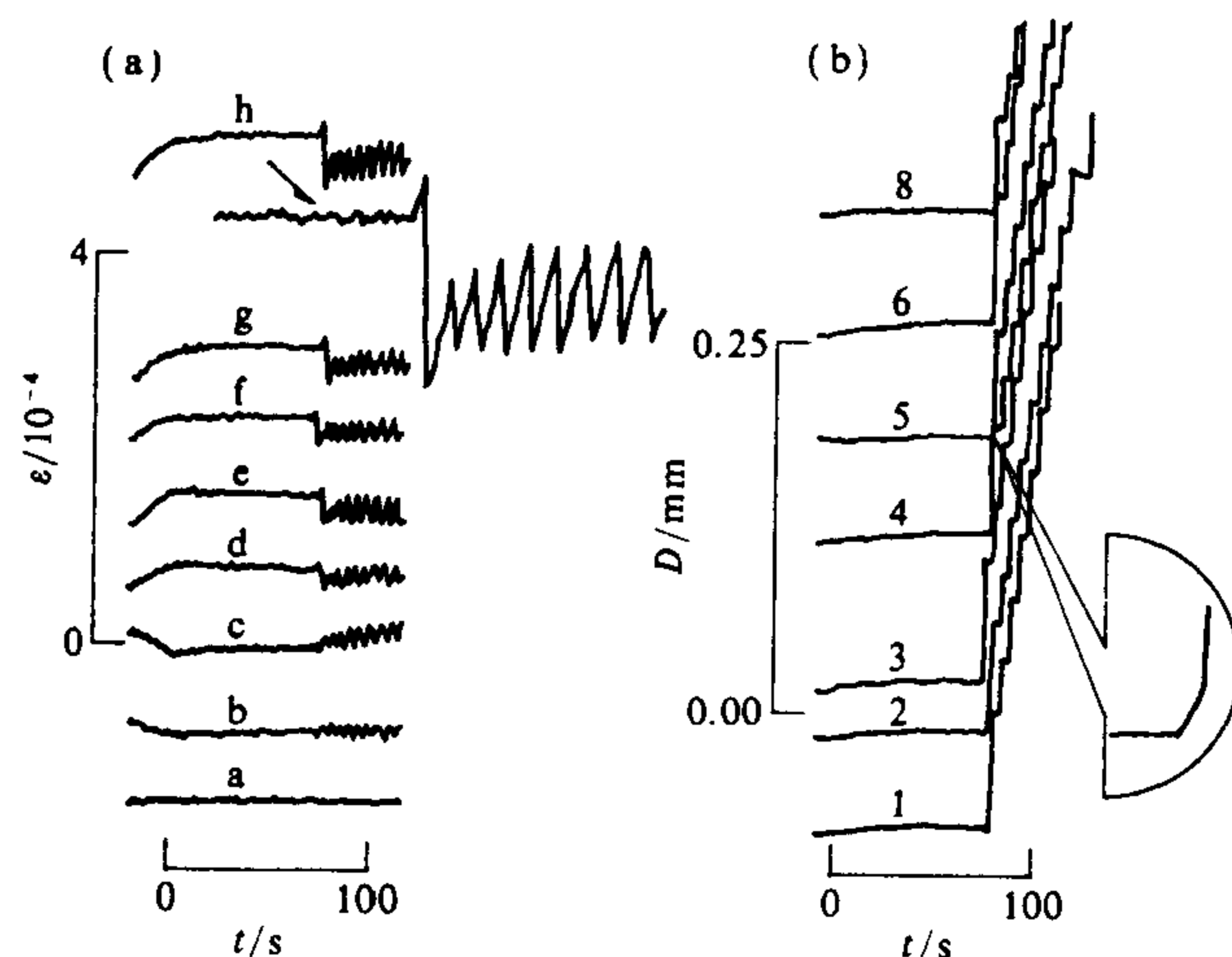


图 2 断层摩擦滑动中另一种粘滑失稳前后应变和断层位移的变化

图 3 是挤压雁列区一条裂纹(I)的快速扩展引起的失稳前后各种观测参量的变化。宏观应力失稳前几十秒加速上升; 断层一些部位位移在失稳时有突变, 但失稳前变化不明显; 由于仪器频响的原因, 声发射主事件可能被漏记, 但从声发射序列来看, 前兆性事件不多, 而类似于余震的事件较多; 失稳时的应变释放主要集中在裂纹处及断层外侧, 失稳前裂纹附近应变下降明显, 而其外应变上升。

混合型失稳 这类失稳见于不连续断层贯通时(如雁列区的贯通)。次级断裂的扩展使得断层非连续部位被贯通, 导致断层发生整体错动而失稳。失稳前兆极为丰富: 源区应变先升后降, 邻区则正相反; 源区断层先闭锁后预滑, 区外断层加速运动; 源区及附近声发射活动频度明显增加。

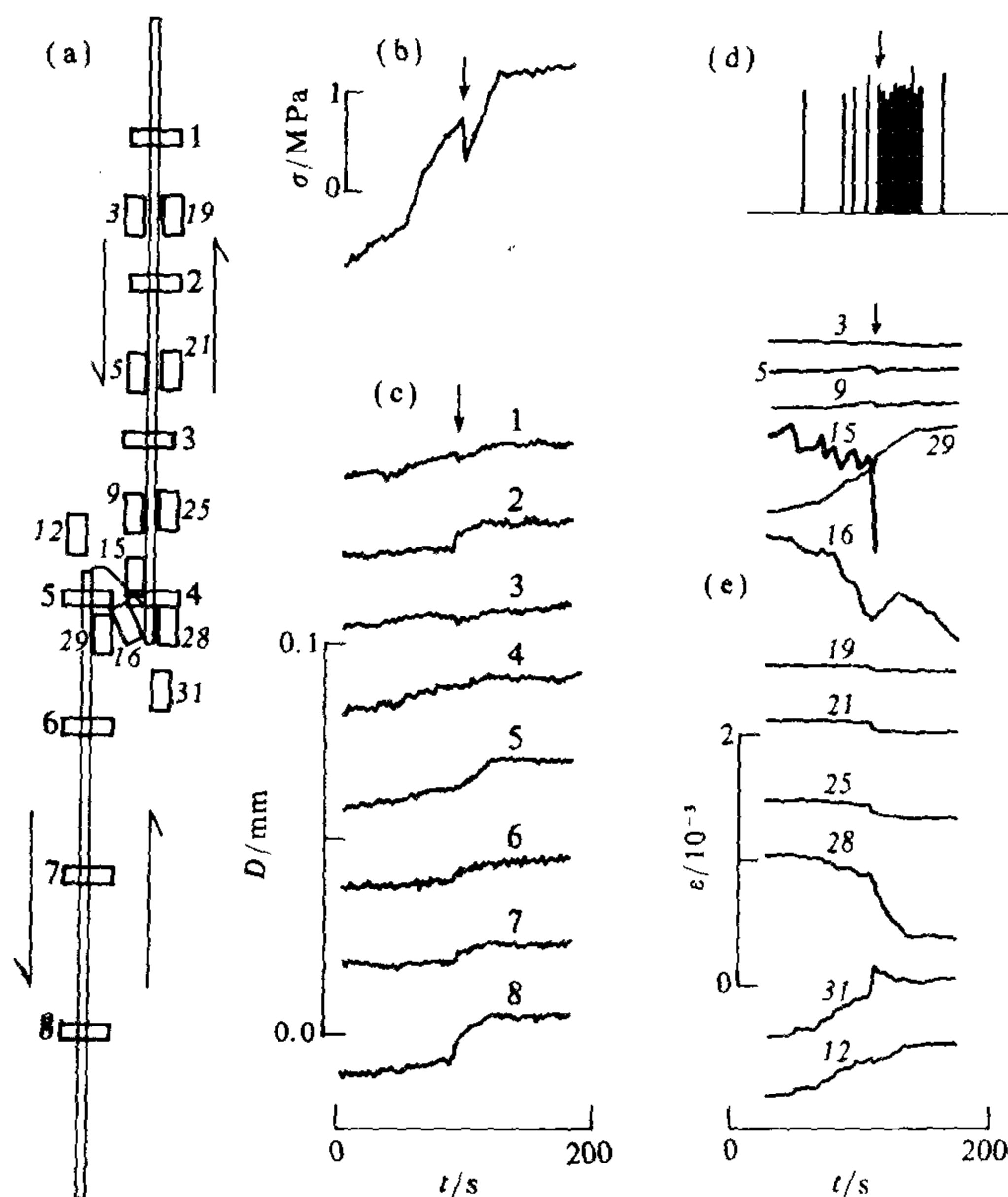


图3 挤压型雁列区破坏过程中一次失稳前后各种观测参数的变化

(a) 断层结构及传感器分布; (b) 应力; (c) 断层位移; (d) 声发射; (e) 应变

图4是挤压型雁列式断层雁列区贯通引起的失稳前后各种观测参数的变化。失稳前约100 s宏观应力开始增加, 紧临失稳下降; 失稳前远离雁列区的段落表现为位移加速, 而靠近雁列区的段落表现为先反向, 后加速; 声发射前兆明显(主事件可能被漏记); 由应变测量结果来看, 失稳发生在裂纹(Ⅰ)的扩展贯通之后, 应变释放区主要为雁列区下部(29号)及外侧(12, 31号), 失稳前这些区域尤其是29号部位应变先加速上升、紧临失稳却较快地下降, 其它部位应变的变化趋势则正相反。

3 讨论

3.1 断层几何结构与地震活动

基于实验结果, 对断层几何结构与地震活动关系简单分析如下:

在较长的平直断层段, 可发生由粘滑引起的强震。其中一类是断层在滑动中局部闭锁, 当应力增加、局部闭锁被打破而发生的失稳。这类地震前在“源区”附近可观察到应变增加、断层位移速率下降、微震活动加强及临近失稳时断层有预滑等前兆现象; 还有一类是断层整体加速滑动或局部加速滑动并沿断层扩展、引起应力下降而造成的失稳, 这类失稳不易观察到前兆。小角度拐折的存在将使其两侧的断层交替成为主导活动构造, 可综合微震活动、断层位移及应变资料来判断。

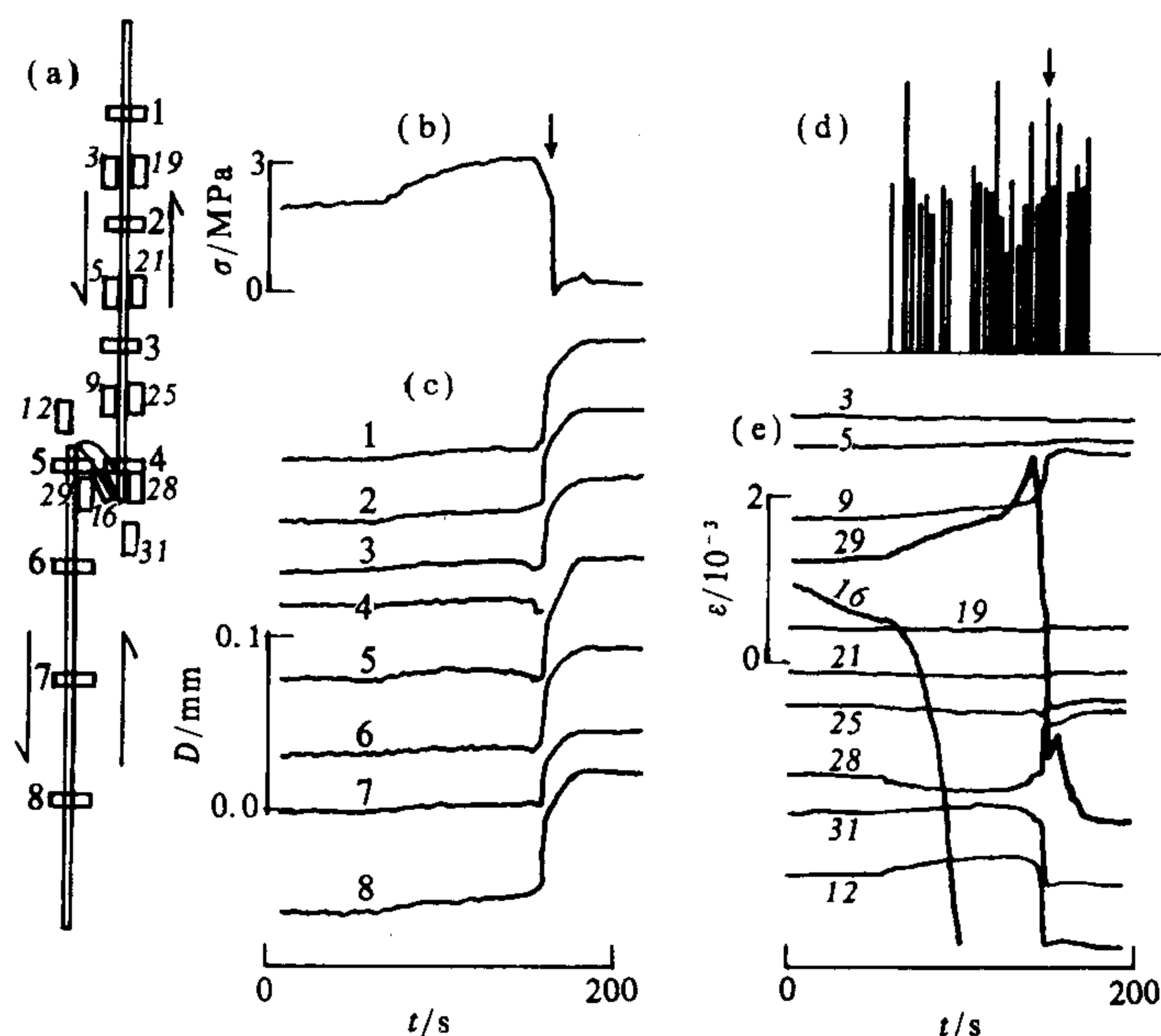


图4 挤压型雁列区贯通失稳前后各种观测参量的变化

(a) 断层结构及传感器分布; (b) 应力; (c) 断层位移; (d) 声发射; (e) 应变

在断层带具有较高强度的非连续部位, 如挤压型雁列区、共线非连通断层非连通区及一些断层交汇部位(杜异军等, 1991), 次级断裂可引起中强地震, 地震前应变场有前兆性变化, 即次级断裂附近(源区)应变明显下降, 邻区应变上升. 而强度较低的非连续部位, 如拉张型雁列区等, 次级破裂仅会引起小地震.

非连续断层的贯通, 如雁列区的贯通、一些“入”字形断层交汇部位的贯通等, 可引起强震. 这类地震前兆现象较为丰富, 总的特点是雁列区或交汇区附近断层闭锁, 区外断层活动加速, 微震活动频度增加; “源区”应变先明显增加, 紧临失稳时下降, 而区外应变变化复杂, 与构造部位有关. 不过, 一些非连续断层贯通强度极高, 如共线非连通断层及某些“入”字形断层交汇部位, 在自然界可能难以完全贯通, 不会发生大震, 但这些部位的微震活动对应力很敏感, 其微震活动的增加可作为区域应力增强的标志.

强度较高的非连续部位的变形对断层带的变形有一定的控制作用, 这些部位的破坏可为两侧断层的滑动失稳提供必要的让位条件. 因此, 一条断裂带地震活跃期可能会从这些部位开始. 另一方面, 这些部位对断层运动有长期的阻碍作用. 因此, 在贯通前和贯通后都可能会阻止发生于其两侧的地震破裂的扩展. 而低强度的非连续部位对断层运动的阻碍作用是暂时的, 只是在其贯通前可能会阻止发生于其两侧的地震破裂的扩展.

实际断层带常是上述典型构造的复杂组合, 在统一的应力作用下必然会表现出复杂的变形和失稳过程, 但在了解构造条件、应力背景的前提下, 通过对实验、野外观测资料的综合分析, 有可能对其未来的变形破坏特征(包括未来的发震地点、失稳类型及相应的前兆场特征)进行分析、推断.

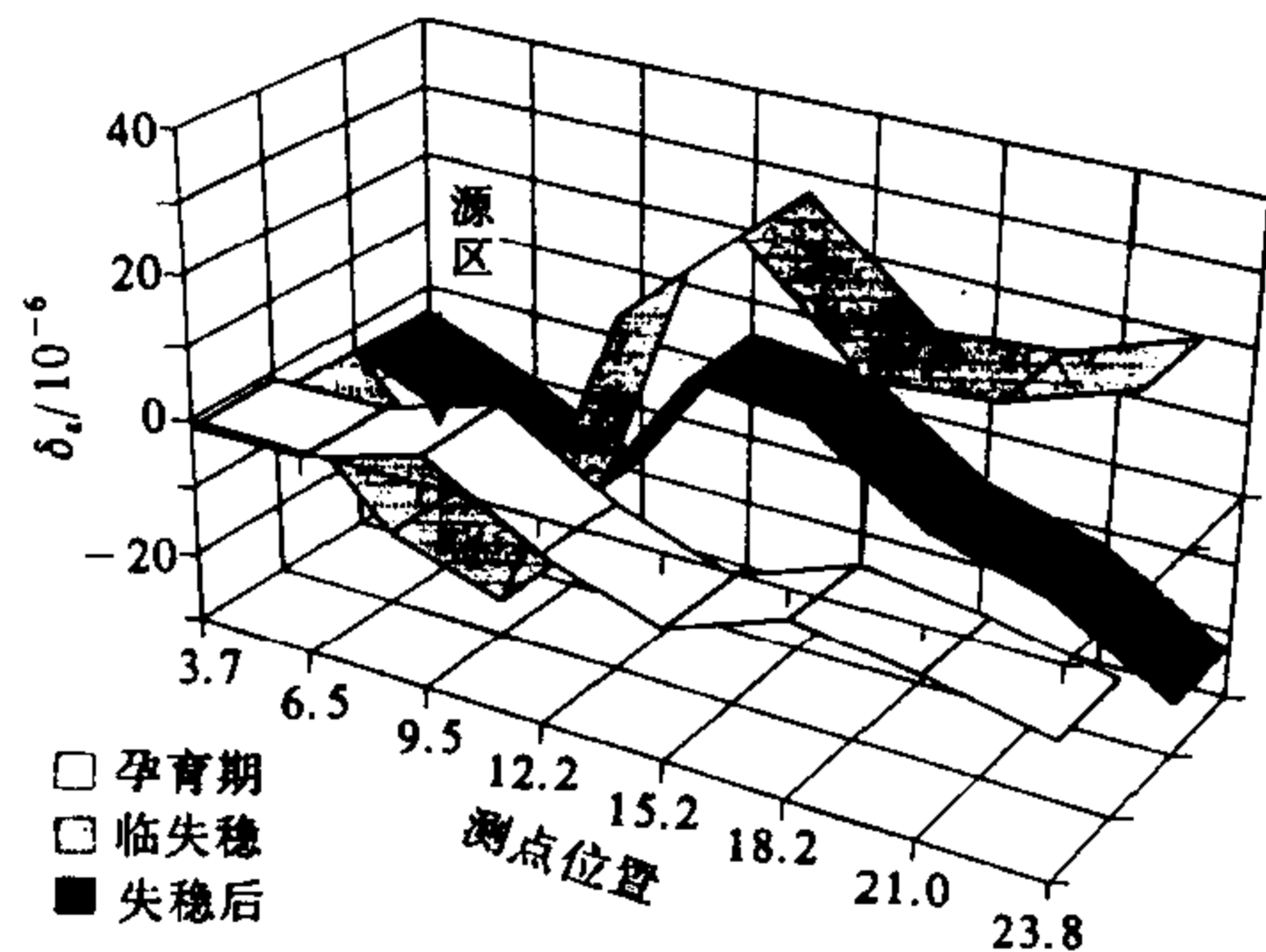


图5 一次粘滑失稳前后平均应变的变化

3.2 地震前兆机理与断层几何

实际震例表明,地震前兆是相当复杂的,“普适性”和“地区性”共存,地震前兆机理仍是有待于探讨的问题(梅世蓉,冯德益,1993).我们根据实验结果对地震前兆机理作一些讨论.

对有应变前兆的粘滑型、混合型失稳事件的分析表明,在失稳孕育过程中,“源区”与邻区存在着应变调整,其特点是“源区”附近在“孕育期”应变增加明显,“临近失稳”前下降;而邻区表现出相反的趋势.从图5所示断层摩擦滑动过程中一次粘滑失稳前后平均应变的变化(相对于失稳前某一时间)可清楚地看出这种特点.这说明应变前兆的产生,实际上是“源区”与邻区相互作用的结果,即失稳前首先是邻区滑动或破裂,应变下降,而“源区”相对闭锁,应变增加;当应变增加到一定程度时,“源区”开始滑动或破裂,应变开始下降.对滑动弱化型粘滑失稳,表现为闭锁区与滑动区的相互作用;对混合型失稳,表现为次级断裂与主断层的相互作用.如果失稳孕育过程中没有这种相互作用,就难以出现应变前兆.由此可见,断层宏观或微观几何结构的不均匀是出现应变前兆的重要条件.

声发射(微震活动)前兆与失稳前“源区”外围应变的释放和临近失稳前“源区”应变的释放有一定的对应关系.不过,应变的释放并不一定都对应有声发射,只有较快的应变释放才会有声发射.在混合型失稳前,与破裂扩展相伴的应变释放和“源区”紧临近失稳前的应变下降均对应有声发射(参见图4);在滑动弱化型粘滑中,失稳前“源区”外断层的活动和

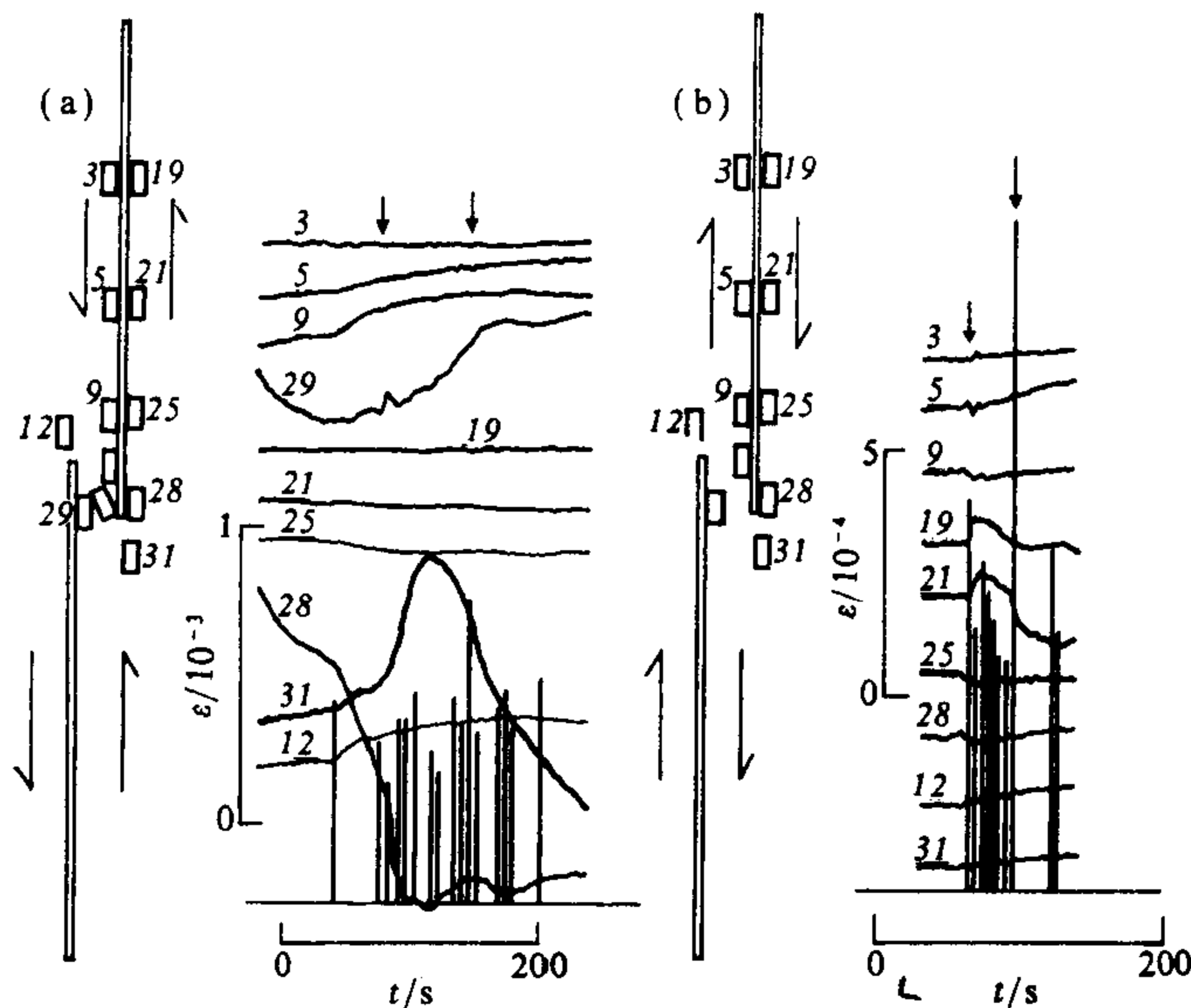


图6 雁列式断层滑动过程中失稳事件前后的声发射和应变变化

(a) 挤压型雁列式断层; (b) 拉张型雁列式断层

“源区”临近失稳时的应变下降也常可引起声发射, 在图 6 所示的雁列式断层滑动过程中, 两次粘滑失稳事件前可清楚地看到这种对应关系. 由此可见, 微震前兆的出现也与构造变形的不均匀有关.

断层位移前兆的出现与几何结构直接相关. 挤压型雁列区次级破裂引起的破裂型失稳无位移前兆, 而两类雁列区完全贯通引起的混合型失稳均有明显的位移前兆; 速度弱化型粘滑失稳位移前兆不明显, 而滑动弱化型粘滑失稳前断层闭锁区预滑明显. 可见, 断层位移前兆实际上是失稳孕育过程中断层运动差异的表现. 因此, 参与失稳的断层几何结构的不均匀有利于位移前兆的出现.

总之, 断层几何结构对地震前兆有重要的影响. 几何结构愈复杂, 参与失稳过程的构造部位愈多, 则前兆种类愈多, 现象愈复杂.

参 考 文 献

- 杜异军, 张大伦, 马瑾, 刘力强, 1991. “入”字型断层的变形与破坏特点. 现代地壳运动研究(5). 北京: 地震出版社. 188~198
- 李建国, 石桂梅, 马瑾, 1989. 雁列裂纹交接区破坏特征与失稳型式研究. 现代地壳运动研究(4). 北京: 地震出版社. 149~155
- 刘力强, 马瑾, 吴秀泉, 1986. 雁列式断层变形与失稳过程的实验研究. 地震学报, 8(4): 393~403
- 马瑾, 1987. 构造物理学概论. 北京: 地震出版社. p. 450
- 梅世蓉, 冯德益, 1993. 中国地震预报概论. 北京: 地震出版社. p. 498
- 张之立, 李强, 1993. 断裂系扩展过程与地球物理场变化特征的实验研究. 地球物理学进展, 8(4): 225~231
- 大中医康, 吉田真吾, 沈林峰, 望月裕峰, 1993. すべり破損核形成過程とMicroseismicity. 日本地震学会講演予稿集(2). 东京: 日本地震学会. p. 298
- 加藤尚之, 佐藤隆司, 山本清彦, 平泽朋郎, 1993. 折れ曲がりのある断層上で発生する多重不安定すべり(1)(2), 日本地震学会講演予稿集(2). 东京: 日本地震学会. p. 296
- 佐藤隆司, 加藤尚之, 雷兴林, 1993. 折れ曲がりのある断層上で発生する多重不安定すべり(1). 日本地震学会講演予稿集(2). 东京: 日本地震学会. p. 295
- Dieterich J C, Barbar D, Conrad G *et al.*, 1978. Slip in a large scale friction experiment. *Proceedings of the 19th U S Rock Mechanics Symposium*. University of Nevada-Reno. 110~117
- Dieterich J C, 1979. Modeling of rock friction: 1. Experimental results and constitutive equations. *J Geophys Res*, 84(B5): 2 161~2 168
- Mogi K, 1984. Fundamental studies on earthquake prediction. *A Collection of Papers of International Symposium on ISCSEP*. Beijing: Seismological Press. 375~402
- Rice J, 1980. The mechanics of earthquake rupture. In: Dziewonski A M and Boschi E (eds), *Physics of the Earth's Interior*. Bologna: Italian Physical Society. 555~569
- Ruina J H, 1983. Slip instability and state variable friction laws. *J Geophys Res*, 91(B9): 9 452~9 472
- Scholz C H, 1990. *The Mechanics of Earthquake and Faulting*. New York: Cambridge University Press. p. 438
- Segall P, Pollard D, 1980. Mechanics of discontinuous faults. *J Geophys Res*, 85(B8): 4 337~4 350
- Sibson R H, 1986. Rupture interaction with fault jogs. In: Das S, Boatright J and Scholz (eds), *Earthquake Source Mechanics*. AGU Geophys Mono, 37: 157~168

青藏高原 Q 值结构反演*

吴建平 曾融生

(中国北京 100081 国家地震局地球物理研究所)

摘要 利用中美合作在青藏高原布设的 11 台 PASSCAL 宽频带数字地震记录的瑞利面波资料,测定了青藏高原东部地区周期为 10~130 s 范围内的平均瑞利波相速度和衰减系数 γ_R ; 反演了该地区地壳、上地幔的平均 S 波速度结构和 Q_β 结构. 结果表明,该地区平均 Q_β 值偏低,并在地壳中存在地震波强吸收层. 地壳中的低 Q_β 层($Q_\beta=93\sim141$)位于 16~42 km 的范围内,它与 S 波低速层(21~51 km)基本一致. 从地壳下部 63 km 后, Q_β 值由 114 随深度逐渐低至上地幔 180 km 处的 34. 由地壳内低速层与低 Q_β 层相对应可以推测,在该深度范围内可能存在岩石的熔融或部分熔融现象. 在反演的 S 波速度结构中,地壳的平均厚度为 71 km, 51 km 处的下地壳存在一明显的速度界面, 96~180 km 处的低速层(4.26 km/s)可能与软流层相对应.

主题词 瑞雷波 相速度 S 波 速度结构 青藏高原 衰减 Q_β 结构

引言

青藏高原是地球上最为特殊的地质单元之一,它是印度次大陆与欧亚大陆碰撞的产物. 该地区地震活动频繁,是研究大陆内地震活动最为重要的地区之一. 爆炸地震、天然地震、重力等观测结果(滕吉文等,1985; 赵珠,曾融生,1992; 丁志锋等,1992)表明,青藏高原地区具有 70 km 的巨厚地壳,地震波速度较其它地区低. 高原南部地热活动强烈(沈显杰等,1985),地壳中存在低速层(陈国英等,1992)及地震波能量的强衰减(冯锐,周海南,1985)等地球物理现象.

对青藏高原进行研究,获得该地区详细的地球物理结构,对了解板块的相互作用过程、青藏高原隆起机制及地震活动机制具有重要的意义. 地震面波的频散特性可以得到地壳、上地幔的 S 波速度结构. 利用青藏高原内部两台站之间的相速度频散特性,将对高原内部的 S 波结构具有更严格的约束(Molnar, 1988). 衰减系数 γ 值的测定,由于受介质横向不均匀引起的散射、聚焦、震型转换等影响较大,采用面波动力学特征很难得到稳定、准确的 Q_β 值结构. 尽管面波 γ 值的测定精度远不如面波群速度、相速度精确,但由于地壳上地幔的非弹性对了解大陆岩石圈的组份、物理性质及状态具有重要意义,它仍是研究某一地区地球物理特性的重要手段之一. Mitchell 和 Xie(1994), Al-Khatib 和 Mitchell(1991)曾对一些大陆地区的面波衰减进行了研究. Singh, Gupta(1982)通过将欧洲大陆作为一个整

* 国家自然科学基金资助项目. 国家地震局地球物理研究所论著 96A0047.
1994-12-21 收到初稿, 1995-05-29 收到修改稿, 1995-06-12 决定采用.

Geometrical textures of faults, evolution of physical field and instability characteristics*

JIN MA (马 瑾), SHENG-LI MA (马胜利), LI-QIANG LIU (刘力强), ZHI-HUI DENG (邓志辉), WEN-TAO MA (马文涛) and TIAN-CHANG LIU (刘天昌)

Institute of Geology, State Seismological Bureau, Beijing 100029, China

Abstract

The spatial and temporal evolution of strain, fault displacement and acoustic emissions during deformation of fault systems with different geometrical textures are studied experimentally under biaxial compression, and the characteristics of typical instability events are analysed. The results show that fault systems with different geometrical textures have different evolutionary images of physical field during deformation. Based on the characteristics of physical field and the deformation mechanism, various types of instability — two types of stick-slip, fracturing type and mixed type instability can be recognized. Different types of instability differ clearly in their precursors, and the instability type is closely related with the geometrical texture and the deformation stage of the fault system. Therefore, it is very significant for earthquake prediction and precursor analysis to investigate the geometrical textures of natural active faults.

Key words: rock mechanical test, fault complex, acoustic emission, strain, fault displacement.

Introduction

Shallow earthquakes are closely related with active faults in the crust. In most cases such a fault is not a simple and continuous surface, but a complicated and discontinuous fault system. It has been shown theoretically that discontinuity in fault geometry may introduce complexity in stress field (Segall and Pollard, 1980). Earthquake cases indicate that nucleation, propagation and termination of an earthquake rupture are often affected by geometrical textures along the fault (Sibson, 1986; Scholz, 1990). Complexity in fault geometry makes deformation process very complicated, which, in turn, leads complexity in distribution of precursors (Ma, 1987). Therefore, it is very significant to study deformation process and evolution of physical field of fault systems with different geometrical textures for understanding earthquake mechanism and precursors. The tectonic deformation rate is usually very slow, so it is difficult to know the evolution process of the deformation and corresponding physical field of a fault system only relying on observation in situ. Laboratory experiments may provide valuable data as reference in this aspect.

Evolution of physical field, such as strain, fault displacement and acoustic emission, has been studied experimentally for simple fault (Dieterich *et al.*, 1978; Mogi, 1984; Ma, 1987), en-echelon faults (Liu *et al.*, 1986; Li *et al.*, 1989; Zhang and Li, 1993), “λ”-shaped faults (Du *et al.*, 1991) and other types of fault complex (Ma, 1987), which has shown the effect of fault

* Received first draft November 3, 1995; Accepted November 14, 1995.

geometry on failure mode and precursor distribution. However, because most experiments were operated under uniaxial loading, they could not fully reveal whole process of deformation for such fault systems. And because recording systems for measurement of physical field in most experiments were analogous ones, measuring accuracy, sampling rate and measuring parameters were limited. Recently some new results have been reported in using multi-channel digital recording system to study physical field (precursor field) during deformation (Ohnaka *et al.*, 1993; Kato *et al.*, 1993; Satoh *et al.*, 1993), but the fault models are rather simple. Therefore, more experimental results are still needed to further understand relationship between geometrical textures of fault and evolution of physical field as well as instability precursors.

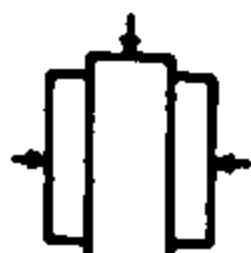
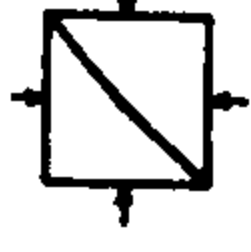
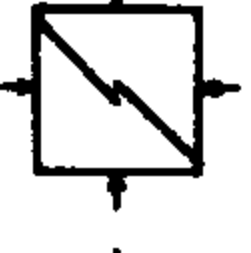
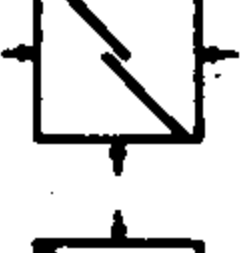
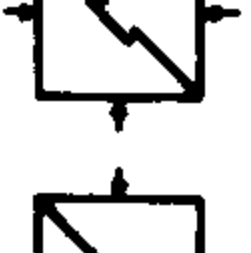

In this paper, several common complexes along strike-slip fault are chosen as experimental models, and the spatial and temporal distributions of strain, fault displacement and acoustic emission (AE) during their deformation under biaxial compression are studied by using a digital recording system with multi-channels, high resolution. The relationship between geometrical textures of fault and instability type as well as precursor characteristics is discussed based on the results.

1 Experimental method

The experiments are operated on a biaxial loading rig, which can be used for double shear, biaxial friction and biaxial compression experiments by changing steel pieces.

Models studied include simple fault, bend fault, compressional, extensional and complex en-echelon faults and co-lined discontinuous faults. Sample feature, experimental type and condition are listed in Table 1.

Table 1 Sample texture and experimental conditions

Fault type	Sample texture	Sample feature	Experimental condition
Simple fault		granodiorite, man-made grinding surface, sliding area is 28 cm × 5 cm	normal stress 5~10 MPa, slip rate 1 μm/s
Bend fault		gabbro, 25 cm × 25 cm × 2 cm, man-made grinding surface 5° bend	lateral stress 5~10 MPa, axial displacement rate 0.5 μm/s
Compressional en-echelon faults		gabbro, 25 cm × 25 cm × 2 cm, jog area 2 cm × 2 cm, width of fault zone 3 mm, filled with plaster	lateral stress 5 MPa, axial displacement rate 0.5 μm/s
Extensional en-echelon faults		<i>idem</i>	<i>idem</i>
Complex en-echelon faults		with two en-echelon jogs, the others are <i>idem</i>	<i>idem</i>
Co-lined discontinuous faults		gabbro, 25 cm × 25 cm × 2 cm, discontinuous segment 2.5 cm, width of fault zone 3 mm, filled with plaster	<i>idem</i>

In the experiments, besides measuring the axial loading and displacement, AE transducers, strain gauges, fault displacement gauges are attached on samples to measure the corresponding physical field.

AE events are recorded by two digital systems with high sampling rate and multi-channels

(total 24 channels). The location of an AE event can be determined by its arriving time from waveforms recorded from different transducers. Its magnitude is determined by using the method in seismology and considering the difference between AE events and earthquakes. In this way, M-t diagram, spatial and temporal distribution of AE events during deformation for each sample can be obtained, and frequency spectrum and focal mechanism of AE events can also be analysed.

The strain is recorded by a digital system with low frequency, high resolution and multi-channels. In the experiments, 32 channels are used for strain measurement, and transducers are standard strain gauges. From measuring record of a strain gauge, the curve of strain vs. time at its position and direction can be obtained directly. The magnitude and direction of planar principal strains and their changes with time at some place can also be obtained by analysing measuring records of a strain pattern composed of three adjacent strain gauges. The fault displacement is measured by the same system with 8 special fault displacement gauges. The fault displacement-time curves at different positions along the fault can be obtained directly from measuring records.

2 Experimental results

2.1 Deformation process and evolution of physical field for typical fault systems

Simple fault The deformation is dominated by sliding along fault surface (with large slip). The accumulation of strain is limited on area near fault surface. AE events are of large magnitude but less numbers relatively. Frictional resistance is steady state in general, and the evolution of physical field is rather stable, and the obvious change can only be observed just before and after instability events.

Bend fault The bend has obvious inhibition on fault movement, and makes two fault segments, with smaller and larger angle to axial direction respectively, become dominative one alternately, which is shown by relatively fast variation in fault displacement, strong accumulation and release of strain near fault, and strong AE activity. AE events are often smaller and with higher main frequency near the bend, but larger and with lower main frequency on straight fault.

En-echelon faults Compressional and extensional en-echelon faults have similar deformation process. The deformation is predominated by fracturing and linking of jogs in the first stage, strain changes intensely but fault slip is quite small, and AE activity has great numbers but low energy. The deformation is predominated by sliding along faults in the second stage, fault slip is large, and strain changes relatively small. However, in the compressional jog, high strain energy can be accumulated and intense release of strain and acoustic emission can be produced, and the jog has a permanent resistance to sliding of faults. But in the extensional jog, rapid release of strain and strong AE event can not be produced, and the jog has almost no resistance to the sliding of fault in the second stage.

The deformation process and the evolution of physical field on complex en-echelon faults are not a simple combination of these two types of en-echelon faults, but contain interaction between them. An interesting phenomenon is that acoustic emission events with high energy occur mostly along main faults near extensional jog with lower stress level, not along faults near compressional jog with higher stress level, but the time of such events is apparently controlled by the deformation process of compressional jog.

Co-lined discontinuous faults The strength is extremely high. Although high stress concentration may occur near fault tips, propagation and linking of such faults are very difficult. The deformation mainly concentrates on discontinuous segment and adjacent faults, which is characterized by great amounts of AE events with low energy.

2.2 Instability type and precursor characteristics

Instability events with different characteristics are observed in the experiments, which can be divided into stick-slip type, fracturing type and mixed type based on their deformation mechanism and evolution characteristics of physical field. Instability is related with geometrical texture, and different type instability differs greatly in precursor characteristics. Based on analysis of typical instability events, the characteristics of each type of instability and precursors are described as follows.

Stick-slip type instability Such type instability occurs in fault sliding and may be seen during sliding of simple fault, bend fault and en-echelon faults after linking of jogs. According to evolution of physical field before and after instability, at least two types of stick-slip instability can be recognized.

The instability process of one type of stick-slip is as follows. During steady-state sliding, fault is locally locked due to change in state of sliding surface, which makes frictional resistance increase. When stress increases to certain level, locked area is broken and unstable slip along fault is caused. Based on constitutive laws of friction, its mechanism may be slip-weakening (Rice, 1980). Precursor characteristics of such kind of instability are: total stress increases; in the vicinity of locked area, strain increases greatly and fault slip rate decreases, but pre-slip can be observed just before instability. Figure 1 shows such an instability event during sliding of simple fault with variations in displacement and strain along fault. Apparently, fault is locked and strain increases before stick-slip and pre-slip occurs just before stick-slip.

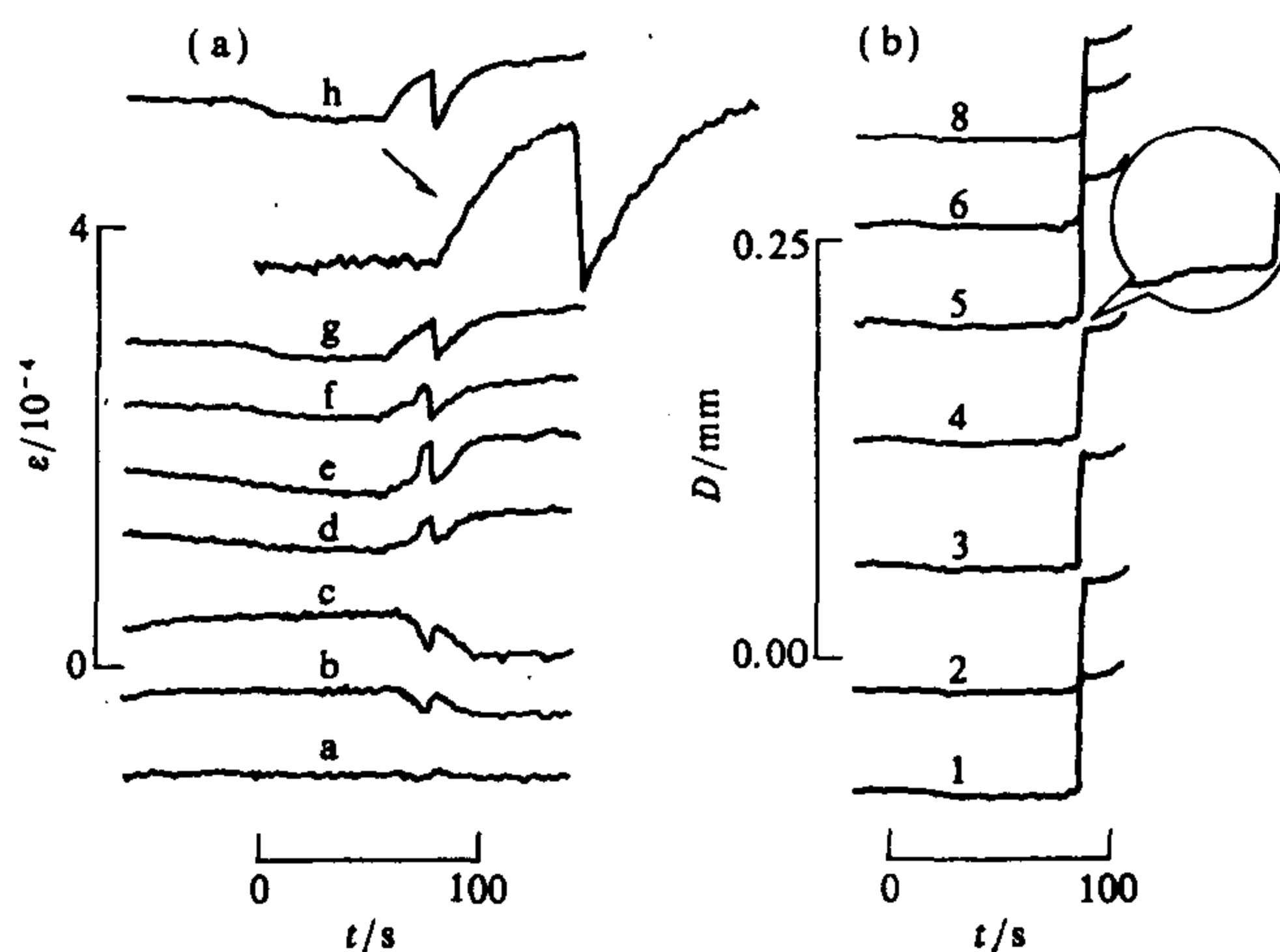


Figure 1 Variations in strain and fault displacement before and after one type of stick-slip instability during fault friction.

The other type of stick-slip occurs because slip rate of whole or partial fault increases and propagates rapidly along fault, which makes stress drop. Its mechanism may be velocity-weakening (Dieterich *et al.*, 1978; Ruina, 1983). It is difficult to detect precursors of such kind of instability. Figure 2 shows such an instability event during sliding of simple fault with variations in displacement and strain along fault. Only instantaneous change in strain can be seen before stick-slip, and fault slip increases rapidly just before stick-slip.

Fracturing type instability It means instability caused by fracturing of discontinuous areas with high strength, which may occur in jog of compressional en-echelon faults and discontinuous

segment of co-lined faults, usually in early stage of deformation. Total stress of fault system increases before instability, and strain decreases obviously in "source area" but increases in area around it just before instability.

Figure 3 shows variations in measuring parameters before and after an instability event caused by rapid propagation of a crack (I) in compressional jog. Total stress begins to increase tens of seconds prior to instability. There are rapid changes in fault displacement associated with the instability in some parts of fault, but change before the instability is not obvious. The major AE event may be lost in record because of the defect in recording system, and the sequence of AE events indicates that there are a few precursory events but a lot of events similar to after-

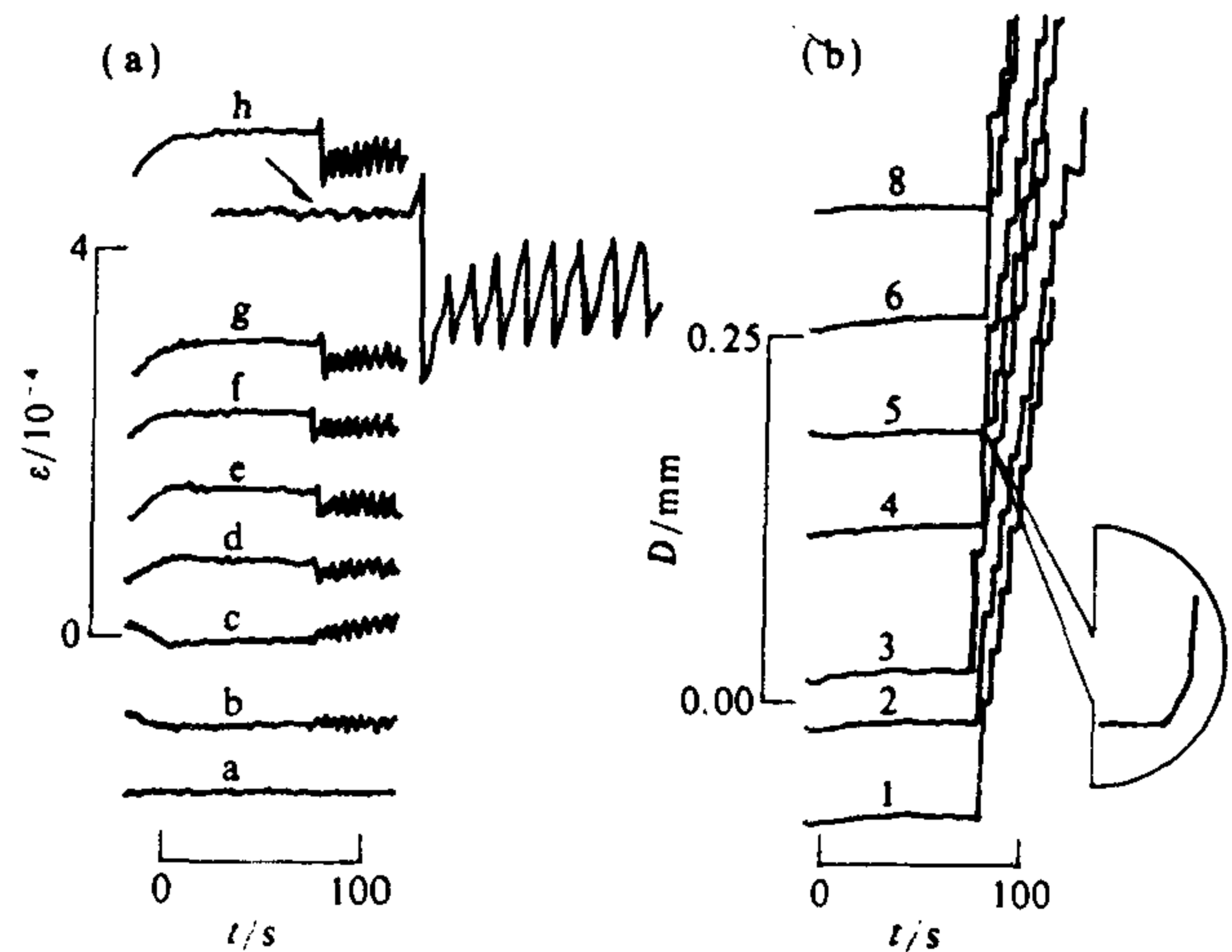


Figure 2 Variations in strain and fault displacement before and after the other type of stick-slip instability during fault friction.

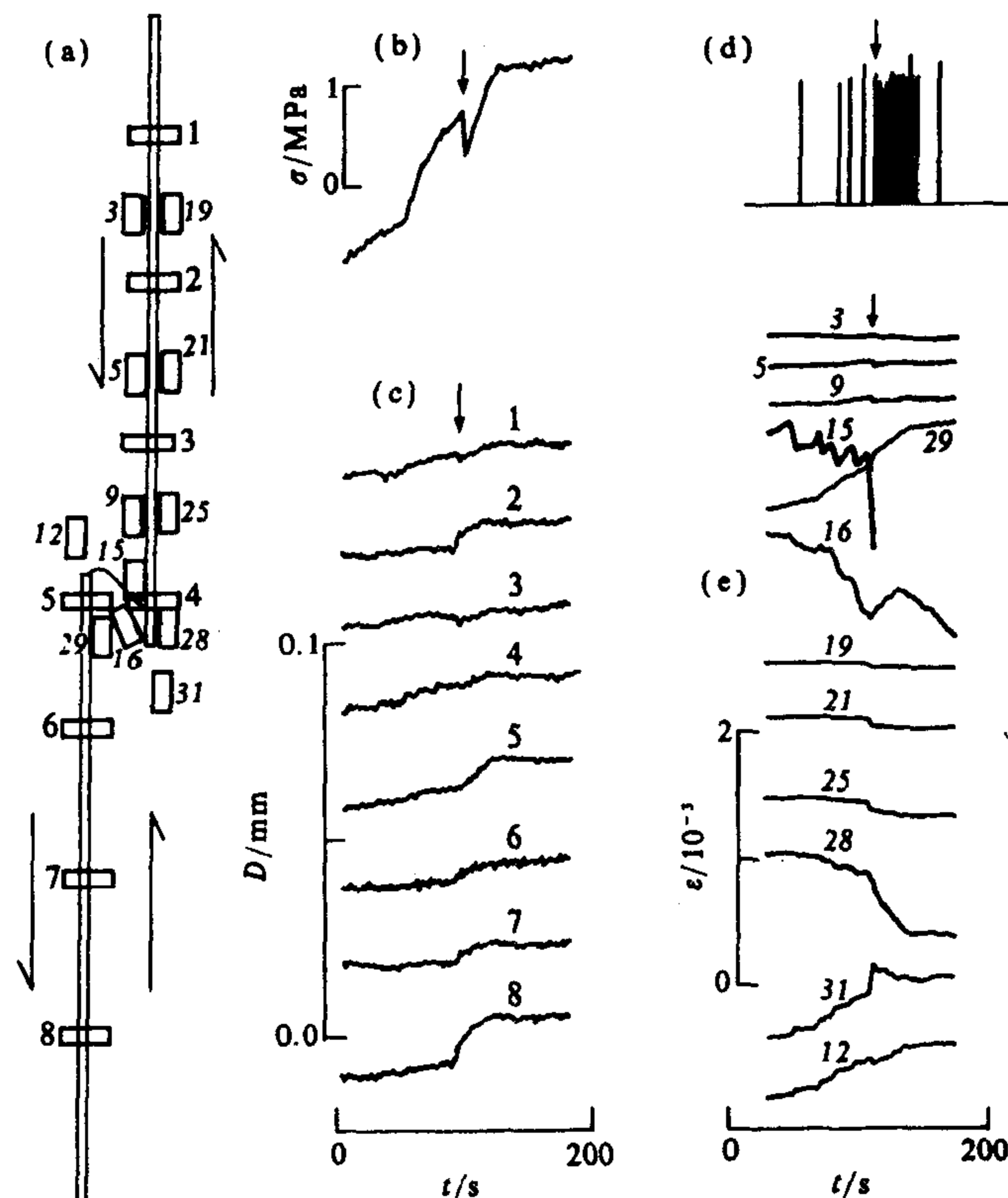


Figure 3 Changes in various parameters before and after an instability event during fracturing of compressional jog. (a) fault texture and distribution of transducers; (b) stress; (c) fault displacement; (d) acoustic emission; (e) strain.

shocks. The strain release associated with instability mainly concentrated on the crack and outside of faults, and the strain decreases clearly near the crack but increases in area off the crack before the instability.

Mixed type instability Such instability involves both fracturing and sliding, and may occur when discontinuous fault system is linked (for example, in linking of jogs along en-echelon faults). Propagation of subfracture makes discontinuous area linked, which leads slip along whole fault system and causes instability. Instability precursors are very rich; strain in "source area" increases first and then decreases, but strain in area around it shows opposite tendency; fault segments near "source area" are locked first and then slip (pre-slip), but fault segments off it slip with faster rate. Acoustic emission activity in the vicinity of "source" becomes frequent.

Figure 4 shows variations in measuring parameters before and after an instability event caused by the linking of jog along compressional en-echelon faults. Total stress begins to increase about 100 s before the instability and decreases just before the instability. Fault segments far-off jog slip acceleratively, while fault segments near jog slip backward first and then acceleratively before the instability. Precursor phenomenon in AE is obvious (the major event may be lost). From the result of strain measurement, it appears that the instability occurs after the linking of a crack (II), and the strain release concentrated on the lower part of jog (No. 29) and its outside (No. 12, 31). Strain in these positions, especially in position No. 29, increases acceleratively before the instability and then decreases rapidly just before the instability, while strain in other areas shows opposite tendency.

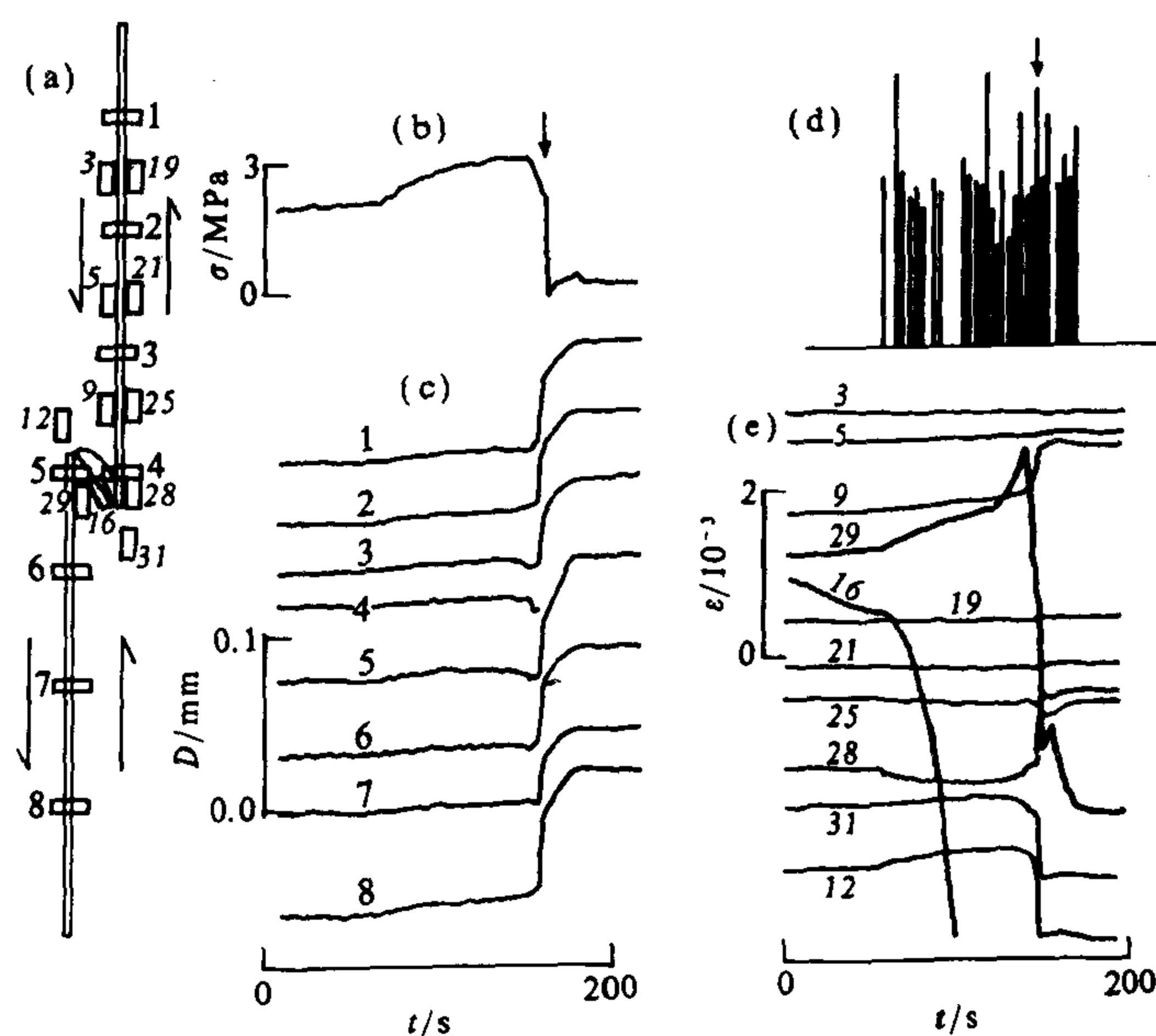


Figure 4 Changes in various parameters before and after instability event caused by linking of compressional jog. (a) fault texture and distribution of transducers; (b) stress; (c) fault displacement; (d) acoustic emission; (e) strain.

3 Conclusions and discussion

3.1 Geometrical textures of fault and seismicity

Based on the experimental results, relationship between geometrical textures of fault and

seismicity is simply analysed as follows.

In straight fault segment with great length, strong earthquakes may occur caused by stick-slip. One type is that fault is locked locally during sliding, and instability is caused when stress increases and the locked area is broken. Before such an earthquake, one may expect to observe increase in strain, decrease in slip rate and intensification in microseismicity near "source area", and pre-slip along fault just before the earthquake. The other type is that whole or partial fault slips accelerating and propagates along fault, which makes stress drop and leads instability. It is difficult to detect precursors of such an earthquake. Existence of bend with small angle along fault makes two fault segments become dominative active structure alternately, which may be recognized according to data of microseismicity, fault displacement and strain.

In discontinuous areas with high strength along fault system, such as compressional jog, discontinuous segment along co-lined faults and some types of fault intersection area (Du, *et al.*, 1991), subfracturing may cause moderate earthquakes. Strain field may have precursory changes before such an earthquake, that is, strain decreases apparently near the subfracture (source area) and increases in area around it. In discontinuous areas with low strength, such as extensional jog, subfracturing may only cause small earthquakes.

Linking of discontinuous faults, such as linking of jogs along en-echelon faults and some intersection areas of "λ" shaped faults, may cause strong earthquakes. Such an earthquake may have very rich precursors. The general characteristics are that fault segments near jog or intersection area are locked, but fault segments off such areas slip acceleratively, and microseismicity intensifies. Strain in "source area" may apparently increase first and then decrease just before the shock, while strain in area around it changes complicatedly, related with structural position. However, some discontinuous areas, such as discontinuous segment of co-lined discontinuous faults and some intersection areas of "λ" shaped fault, are too strong to link in nature, and they may not cause strong earthquakes at all. But microseismicity in such areas is very sensitive to stress, so microseismicity in such areas may be taken as indicator of regional stress.

Discontinuous areas with high strength may play role in controlling deformation along the whole fault system. Deformation and failure of such areas can provide yielding condition necessary for slip instability along faults, so an seismo-active period along a fault system may begin from such areas. In addition, such area may have resistance to fault movement for a long time, so it may inhibit propagation of earthquake rupture initiated from its either side both before and after it is linked. In contradiction, discontinuous area with low strength may have resistance to fault movement for a short time, it can inhibit earthquake rupture only before it is linked.

A natural fault system is often a complicated complex of typical textures described above, and must show complicated process of deformation and instability under the identical stress field. But on the premise of understanding tectonic and stress background, its possible deformation and failure characteristics (including sites and magnitude of potential earthquakes, instability type and corresponding precursors) may be analysed and estimated by summarizing experiment results and measurement data *in situ*.

3.2 Mechanism of earthquake precursors and fault geometry

Earthquake cases indicates that earthquake precursors are very complicated, and both "universality" and "regionality" exist at the same time, and mechanism of earthquake precursors is still needed to explore. Here we try to discuss this question based on the experimental results.

The analysis on stick-slip type instability with strain precursor and mixed type instability shows that there is adjustment in strain between "source area" and area around it during pre-rupture process of an instability event, and the characteristics are that strain in "source area" in-

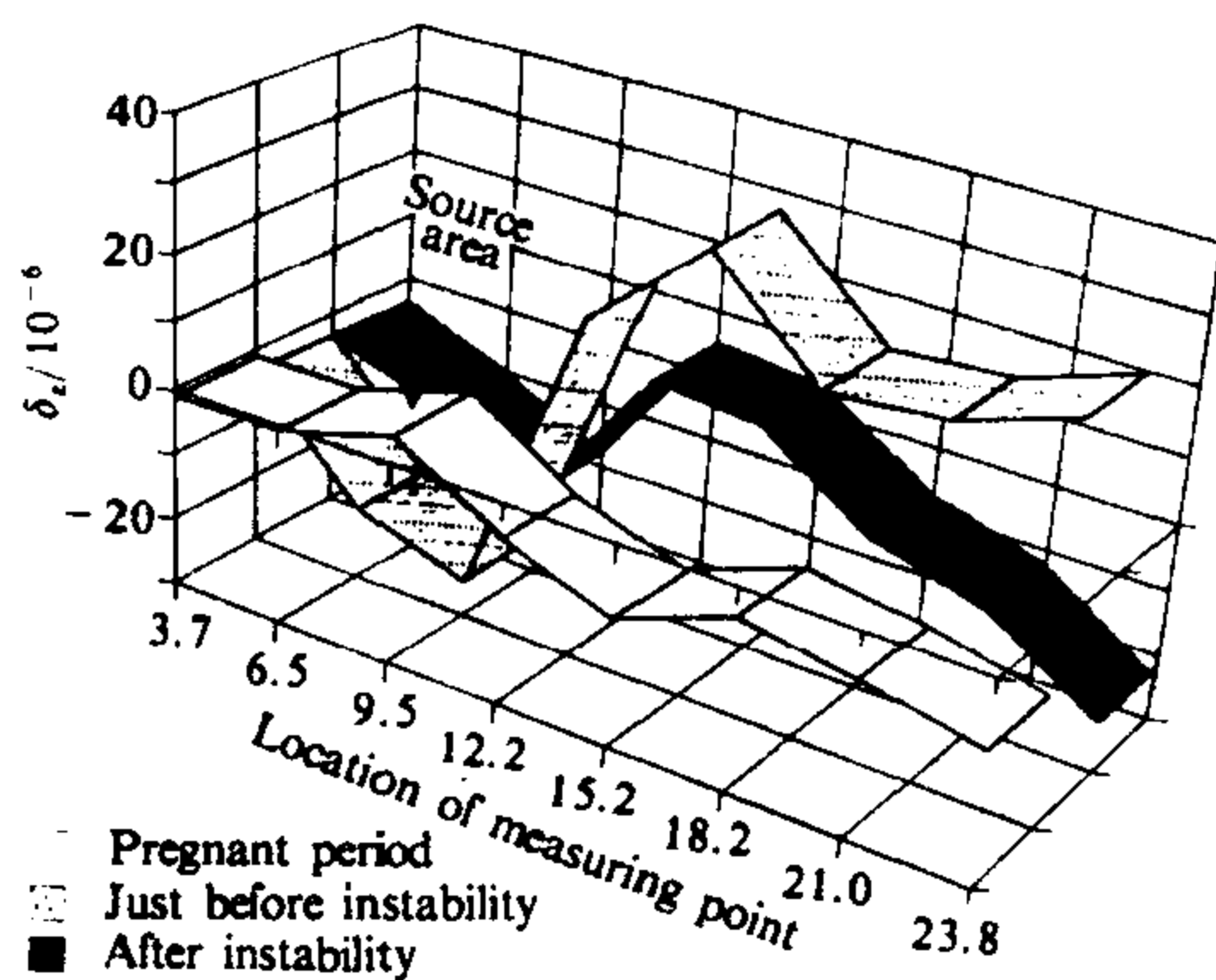


Figure 5 Changes in mean strain before and after a stick-slip.

increases apparently during “pregnant period” and decreases “just before instability”, but it presents opposite tendency in area around it. Such characteristics can be clearly seen from the changes in mean strain before and after a stick-slip instability during fault friction shown in Figure 5. This indicates that the occurrence of strain precursor is the result of interaction between “source area” and area around it. Before instability, area around “source” slips or fractures first and strain decreases, while “source area” is locked relatively and strain increases. When strain increases to some level, “source area” begins to slip or fracture and strain begins to decrease. Such interaction exists between locked region and slip region for stick-slip instability caused by slip-weakening, and

between subfracture and main fault for mixed type instability. If there is no such interaction, it will be difficult for strain precursor to occur.

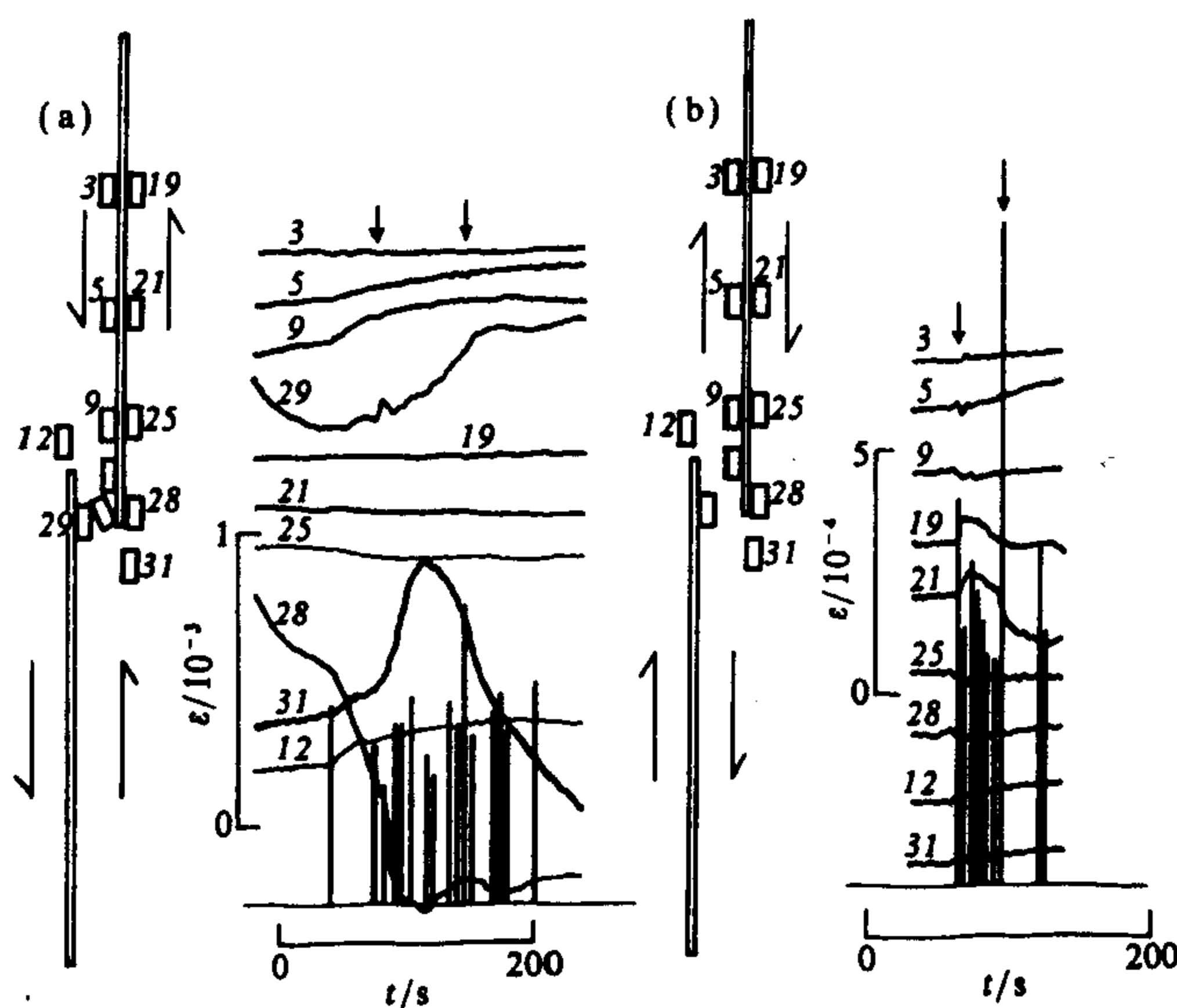


Figure 6 Variations in AE and strain before and after instability events during sliding of en-echelon faults. (a) compressional en-echelon faults; (b) extensional en-echelon faults.

AE (microseismicity) precursor is related with strain release in area around “source” before instability and in “source area” just before instability. But strain release is not always associated with AE activity, only rapid strain release is associated with AE activity. For mixed type instability, strain release associated with fracture propagation before instability and strain decreasing in “source area” just before instability are corresponding with AE activity (see Figure 4). For stick-slip instability caused by slip weakening, strain release along fault off “source area” before instability and in “source area” just before instability can also produce AE activity. Such relationship can be seen before two stick-slip instability events during sliding of en-echelon faults shown